

This is a repository copy of *A novel stibacarbaborane cluster with adjacent antimony atoms exhibiting unique pnictogen bond formation that dominates its crystal packing.*

White Rose Research Online URL for this paper:

<https://eprints.whiterose.ac.uk/121161/>

Version: Accepted Version

---

**Article:**

Holub, Josef, Melichar, Petr, Růžičková, Zdeňka et al. (5 more authors) (2017) A novel stibacarbaborane cluster with adjacent antimony atoms exhibiting unique pnictogen bond formation that dominates its crystal packing. Dalton Transactions. pp. 13714-13719. ISSN 1477-9234

<https://doi.org/10.1039/c7dt02845h>

---

**Reuse**

Items deposited in White Rose Research Online are protected by copyright, with all rights reserved unless indicated otherwise. They may be downloaded and/or printed for private study, or other acts as permitted by national copyright laws. The publisher or other rights holders may allow further reproduction and re-use of the full text version. This is indicated by the licence information on the White Rose Research Online record for the item.

**Takedown**

If you consider content in White Rose Research Online to be in breach of UK law, please notify us by emailing [eprints@whiterose.ac.uk](mailto:eprints@whiterose.ac.uk) including the URL of the record and the reason for the withdrawal request.

# A novel stibacarbaborane cluster with adjacent antimony atoms exhibiting unique pnictogen bond formation that dominates its crystal packing

Josef Holub,<sup>a</sup> Petr Melichar,<sup>b</sup> Zdeňka Ružičková,<sup>c</sup> Jan Vrána,<sup>c</sup> Derek A. Wann,<sup>d</sup> Jindřich Fanfrlík,<sup>b\*</sup> Drahomír Hnyk,<sup>a\*</sup> and Aleš Ružička<sup>c\*</sup>

<sup>a</sup> Institute of Inorganic Chemistry of the Czech Academy of Sciences, v.v.i. 250 68 Husinec-Řež, Czech Republic. E-mail: [hnyk@iic.cas.cz](mailto:hnyk@iic.cas.cz)

<sup>b</sup> Institute of Organic Chemistry and Biochemistry of the Czech Academy of Sciences, Flemingovo nám. 2, 166 10 Prague 6, Czech Republic. Email: [fanfrlik@uochb.cas.cz](mailto:fanfrlik@uochb.cas.cz)

<sup>c</sup> Department of General and Inorganic Chemistry, Faculty of Chemical Technology, University of Pardubice, Studentská 573, 53210 Pardubice, Czech Republic. Email: [ales.ruzicka@upce.cz](mailto:ales.ruzicka@upce.cz)

<sup>d</sup> Department of Chemistry, University of York, Heslington, York, UK YO10 5DD

## Abstract

We have prepared *nido*-7,8,9,11-Sb<sub>2</sub>C<sub>2</sub>B<sub>7</sub>H<sub>9</sub>, the first cluster with simultaneous Sb-B, Sb-C and Sb-Sb atom pairs with interatomic separations with magnitudes that approach the respective sums of covalent radii. However, the length of the Sb-Sb interaction in this cluster is slightly less than the sum of the covalent radii. Quantum chemical analysis has revealed that the crystal packing of *nido*-7,8,9,11-Sb<sub>2</sub>C<sub>2</sub>B<sub>7</sub>H<sub>9</sub> is predominantly dictated by pnictogen bonding, an unconventional  $\sigma$ -hole interaction. Indeed, the interaction energy of a very strong Sb<sub>2</sub>⋯H-B Pn-bond in the *nido*-7,8,9,11-Sb<sub>2</sub>C<sub>2</sub>B<sub>7</sub>H<sub>9</sub> dimer exceeds  $-6.0$  kcal mol<sup>-1</sup>. This is a very large value and is comparable to the strengths of known Pn-bonds in Cl<sub>3</sub>Pn⋯ $\pi$  complexes (Pn = As, Sb).

## Introduction

Boron atoms have a remarkable ability to form 3-center-2-electron (3c2e) bonds, which results in astonishing variety of stable three-dimensional molecular structures composed of triangular B-B-B and B-H-B faces.<sup>1,2</sup> An important class of boranes comprises *closo*-B<sub>n</sub>H<sub>n</sub><sup>2-</sup> and *nido*-B<sub>n</sub>H<sub>n</sub><sup>4-</sup>. BH vertices can be formally replaced by CH<sup>+</sup>, S<sup>2+</sup>, Se<sup>2+</sup>, P<sup>+</sup>, As<sup>+</sup> and Sb<sup>+</sup> units which results in a variety of heteroboranes. While carboranes and thaboranes are common, heteroboranes with heavier main group

elements are rare. The first Sb-containing boron clusters to be synthesized were *closo*-1,2-AsSbB<sub>10</sub>H<sub>10</sub>, *closo*-1,2-Sb<sub>2</sub>-B<sub>10</sub>H<sub>10</sub> and *nido*-7,8-SbCB<sub>9</sub>H<sub>11</sub><sup>-</sup> although no crystal structures could be determined.<sup>3</sup> The *closo*-1,2-Sb<sub>2</sub>B<sub>10</sub>H<sub>10</sub> compound subsequently allowed a bis(phosphine)metalladistibaborane to be synthesized and crystallized.<sup>4</sup> However, the Sb<sub>2</sub>B<sub>3</sub> pentagonal belt was stabilized by Pd in this cluster. It is often the case that slightly unstable arrangements are capped with a metal atom to help their stabilization.<sup>5</sup> Inspired by 3-Cl-*nido*-7,8,9,11-P<sub>2</sub>C<sub>2</sub>B<sub>7</sub>H<sub>9</sub> (**1**) and 3-I-*nido*-7,8,9,11-As<sub>2</sub>C<sub>2</sub>B<sub>7</sub>H<sub>9</sub> (**2**) compounds,<sup>6,7</sup> we have succeeded for the first time in generating a pentagonal belt containing two Sb atoms without having to cap it with a metal atom *nido*-7,8,9,11-Sb<sub>2</sub>C<sub>2</sub>B<sub>7</sub>H<sub>9</sub> (**3**, see Fig. 1).

Nowadays, particular attention is paid to  $\sigma$ -hole noncovalent interactions.<sup>8</sup> The  $\sigma$ -holes are defined as positive electrostatic potential (ESP) areas capable of interacting with electron-rich regions.<sup>9</sup> They are most often located along the vector of a covalent bond to a halogen (X), chalcogen (Y), or pnictogen (Pn) atom. Consequently,  $\sigma$ -hole interactions are often called X-, Y- or Pn-bonds. These interactions are well known in organic chemistry. A  $\sigma$ -hole is most often characterized by its magnitude ( $V_{s,max}$ ); the higher the  $V_{s,max}$  value, the stronger the X-bond. The  $V_{s,max}$  value can be increased by increasing the atomic number of the X atom or by changing the chemical environment. Recently,  $\sigma$ -hole interactions within heteroboranes with positive  $\sigma$ -holes on heteroatoms incorporated have received attention, resulting in remarkably strong  $\sigma$ -hole interactions.<sup>10</sup> This is counterintuitive when one considers the very low electronegativity of B atoms. It was a phenyl-*exo*-substituted thiaborane molecule where the  $\sigma$ -hole interactions were first noticed with the resulting formation of a Y-bond that was responsible for the overall packing motif in the crystal structure.<sup>10a</sup> A strong X-bond has been observed in the crystal packing of Br-*exo*-substituted carbaborane.<sup>11</sup> Although a series of heteroboranes containing Pn atoms is already known experimentally such as **1** and **2**,<sup>6</sup> no experimental evidence for Pn-bonding in heteroboranes has been reported. Therefore, we used **3** to validate the ability of heteroboranes to form noncovalent Pn-bonds.

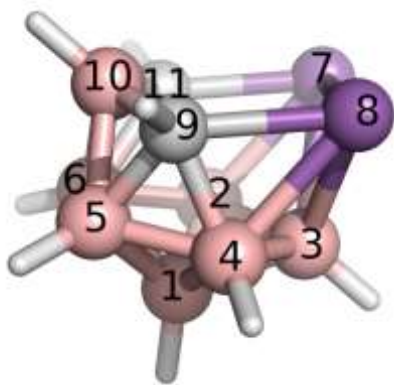


**Figure 1.** The molecular structure and atomic numbering of *nido*-7,8,9,11-Sb<sub>2</sub>C<sub>2</sub>B<sub>7</sub>H<sub>9</sub>, **3**.

## Results and discussion

### Structural characterization by NMR

The properties of **3** can be inferred from NMR experiments and QM calculations. Table 1 compares experimental and computed <sup>11</sup>B NMR chemical shifts, showing excellent agreement between the experimental and computed NMR values with the exception of B(5,6), which are antipodally coupled<sup>12</sup> to the Sb atoms. The discrepancy, which is not unusual for the third row and other heavier elements,<sup>12</sup> indicates that B(5,6) atoms are strongly influenced by Sb(7,8).

Aromatic ring currents are observed in 2D and 3D aromatic molecules such as benzene and *closo*-B<sub>12</sub>H<sub>12</sub><sup>2-</sup>. The nucleus-independent chemical shift (NICS) is a computational method that expresses the absolute magnetic shielding at the center of a 2D or 3D molecule. The NICS values<sup>13</sup> for various parts of molecule **3** are computed to be -41.7, -44.5, -41.7, -44.9, -22.5 and -17.4 ppm for the Sb-B-B, B-B-B, Sb-Sb-B, Sb-B-C triangles, center of the molecule, and open pentagonal belt, respectively. These results indicate that the cluster as a whole is of an aromatic nature. The fact that the triangles that are closest to antimony are highly aromatic indicates that the Sb atoms donate valence electrons to the corresponding atomic triangles. Even the NICS values that are less negative than -40 ppm are comparable to the aromaticity displayed by the 1,3-dehydro-5,7-adamantanediyl dication and *closo*-B<sub>12</sub>H<sub>12</sub><sup>2-</sup> (NICS values of -49.6 and -34.4 ppm, respectively).<sup>13</sup> The NICS value for the Sb-Sb-C-B-C pentagon of -17.4 ppm is comparable to the values associated with pyrrole and thiophene (NICS values of -17.3 and -14.7 ppm, respectively; more details in Ref. 13). The 7,8,9,11-Pn<sub>2</sub>C<sub>2</sub>B<sub>7</sub>H<sub>9</sub> (Pn = P, As) compounds display similar trends of NICS values.

**Table 1.** NMR results for **3**.<sup>a</sup>

	B(1)	B(3)	B(2,4)	B(10)	B(5,6)
GIAO <sup>b</sup>	-29.3	-15.5	-6.5	-0.4	1.6
Exp.	-30.2	-16.8	-9.2	-1.5	-6.9

<sup>a</sup> All in ppm with respect to BF<sub>3</sub>.OEt<sub>2</sub>. Atomic numbering shown in Fig. 1.

<sup>b</sup> GIAO-MP2/II(def2-TZVP+ECP on Sb)//MP2/cc-pVTZ(def2-TZVP+ECP on Sb).

### Crystal structure of **3**

In the crystal structure of **3** (see Fig. 2), four molecules were found in the chiral unit cell. A striking feature of this structure is the well-determined Sb-Sb separation (2.7546(6) Å), which seems to be in line with analogous distances in reduced or over-reduced Sb compounds containing two or more metal atoms. There are several different classes of compound that could be used for comparison where the Sb-Sb distances are a bit longer than the sum of the covalent radii of 2.8 Å.<sup>14a</sup>

Complexes with a Sb-B and Sb-C bonds in a single molecule are very rare.<sup>14b,14c</sup> The reported Sb-C separation of **3** is elongated by *ca.* 0.07 Å when compared to typical C(aromatic)-SbIII distance. Similarly, the Sb-B distances in **3** (range from 2.312 to 2.458 Å) approach the sum of the covalent radii of the constituent atoms, i.e. 2.25 Å.<sup>14a</sup>

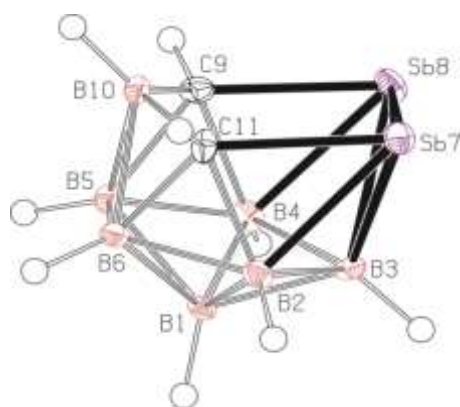


**Figure 2.** The molecular structure (ORTEP 50% probability level) and atomic numbering of **3**. Selected interatomic distances [Å] and angles [°]: Sb7-Sb8 2.7546(6), Sb7-C11 2.225(8), Sb8-C9 2.217(8), C9-B10 1.611(11), B10-C11 1.603(11), B2-Sb7 2.326(9), B3-Sb7 2.458(8), B3-Sb8 2.446(7), Sb8-B4 2.313(8); C9-Sb8-Sb7 89.8(2), C11-Sb7-Sb8 90.61(19), B10-C11-Sb7 115.7(5), B10-C9-Sb8 116.9(5), C11-B10-C9 119.2(6), C9-Sb8-B4 44.5(3), C9-Sb8-B3 77.0(3), B4-Sb8-B3 45.8(3), B4-Sb8-Sb7 92.17(19), B3-Sb8-Sb7 56.03(19), C11-Sb7-B2 44.0(3), C11-Sb7-B3 76.8(3), B2-Sb7-B3 46.1(3), B2-Sb7-Sb8 92.4(2), B3-Sb7-Sb8 55.62(17).

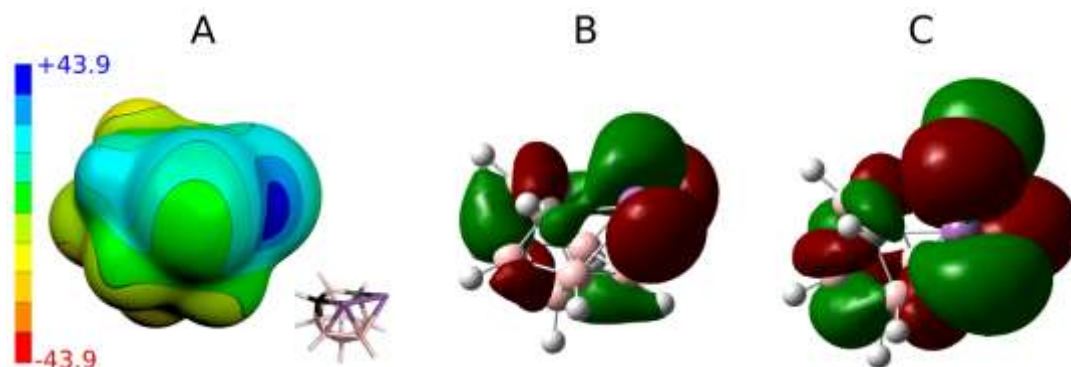
### Electrostatic potential (ESP) analysis

In order to understand Pn-bonding more generally, we analyzed the charge distributions for a series of  $\text{PnCl}_3$  and *nido*- $\text{Pn}_2\text{C}_2\text{B}_7\text{H}_9$  (Pn = P, As, and Sb) molecules. The computed  $V_{s,\text{max}}$  and  $\mu$  values are summarized in Table 2. Sb has very low electronegativity comparable to that of B but considerably smaller than those values for C and Cl. In accordance with the concept of electronegativity, Sb atom has highly positive  $V_{s,\text{max}}$  values in  $\text{SbCl}_3$  of  $48.6 \text{ kcal mol}^{-1}$ . However, the Sb atoms in **3** also has very high  $V_{s,\text{max}}$  value of  $42.7 \text{ kcal mol}^{-1}$  (the  $\sigma$ -hole in-between the adjacent Sb atoms; see Fig. 3) despite being bonded to B and C atoms, which are considerably less electronegative than Cl atoms. Interestingly, the Sb vertices have more positive ESP surfaces than the CH vertices (see Fig. 3) and the Sb atoms lie at the center of a partial positive charge within **3**. A very large dipole moment ( $\mu$ ) of **3** ( $\mu$  of 4.0 D) also confirms that the center of the Sb-Sb vector is positively charged.

**Table 2.** Magnitude of  $\sigma$ -holes ( $V_{s,\text{max}}$ ) on the surfaces of Group V and VII atoms and dipole moments ( $\mu$ ) computed at the HF/cc-pVDZ level in various pnictogen compounds.

	$V_{s,\text{max}} / \text{kcal mol}^{-1}$		$\mu / \text{D}$
	Group V atoms	Group VII atoms	
$\text{PCl}_3$	$3 \times 29.2$	$3 \times 6.7$	1.1
$\text{AsCl}_3$	$3 \times 38.6$	$3 \times 2.9$	2.1
$\text{SbCl}_3$	$3 \times 48.6$	$3 \times -3.3$	3.3
<i>nido</i> -7,8,9,11- $\text{P}_2\text{C}_2\text{B}_7\text{H}_9$ ( <b>1</b> )	24.8	—	2.0
3-Cl- <i>nido</i> -7,8,9,11- $\text{P}_2\text{C}_2\text{B}_7\text{H}_9$	25.4	-3.1	2.8
<i>nido</i> -7,8,9,11- $\text{As}_2\text{C}_2\text{B}_7\text{H}_9$	31.1 and $2 \times 24.4$	—	2.8
3-I- <i>nido</i> -7,8,9,11- $\text{As}_2\text{C}_2\text{B}_7\text{H}_9$ ( <b>2</b> )	32.2 and $2 \times 29.0$	8.2	3.5
<i>nido</i> -7,8,9,11- $\text{Sb}_2\text{C}_2\text{B}_7\text{H}_9$ ( <b>3</b> )	$1 \times 42.7$ and $2 \times 25.7$	—	4.0

**Figure 3.** Computed electrostatic potential (ESP) surface for compound **3** (A). The color range of the ESP in kcal mol<sup>-1</sup>. The HOMO (B) and LUMO (C) of **3** were derived at the same level of theory as ESP, see computational modeling.



### Crystal packing and noncovalent interactions

We have studied pairwise interactions in the crystal structure of **3**. It was not possible to compare these interactions to the parent *nido*-7,8,9,11-Pn<sub>2</sub>C<sub>2</sub>B<sub>7</sub>H<sub>9</sub> (Pn = P, As) complexes, as its reveal poor quality crystals, which prevents them from performing reliable X-ray structure determination. Hence, we opted for the halogenated analogues of **1** and **2**, for which the crystal structures had already been determined.<sup>6,7</sup> We performed highly accurate PM2.5/CBS calculations for all of the bonding motifs as well as benchmark CCSD(T)/CBS calculations. All the computed interaction energies ( $\Delta E$ ) are summarized in Table 3 (see also Fig. 4). Each molecule of **1** makes two Pn-bonds (P<sub>2</sub>···H-B and P<sub>2</sub>···Cl-B). These two Pn-bonds form the A···B binding motif which has  $\Delta E$  of -6.1 kcal mol<sup>-1</sup> and was the dominant binding motif for **1**. Besides Pn-bonding, molecule **1** also forms a CH···Cl-B H-bond and a C-H···B-H HH-bond. The H-bonding of **1** is, however, weaker than its Pn-bonding and the  $\Delta E$  of the A···C motif is less negative (-4.4 kcal mol<sup>-1</sup>).

The crystal packing of **2** is also dominated by Pn-bonding, as the binding motifs with most negative  $\Delta E$  values are stabilized by Pn-bonding. The A···B motif of **2** is stabilized by two symmetrical As<sub>2</sub>···H-B Pn-bonds and has  $\Delta E$  of -6.0 kcal mol<sup>-1</sup>. An estimated  $\Delta E$  of this isolated Pn-bond would thus be about -3 kcal mol<sup>-1</sup>. The A···C motif of **2** has comparable  $\Delta E$  of -5.7 kcal mol<sup>-1</sup> and is stabilized by As···H-B and As···I-B Pn-bonds. The other motifs

have less negative  $\Delta E$  values. Among them the most negative is the D $\cdots$ E motif with two As $\cdots$ H-B Pn-bonds and  $\Delta E$  of  $-4.5 \text{ kcal mol}^{-1}$ .

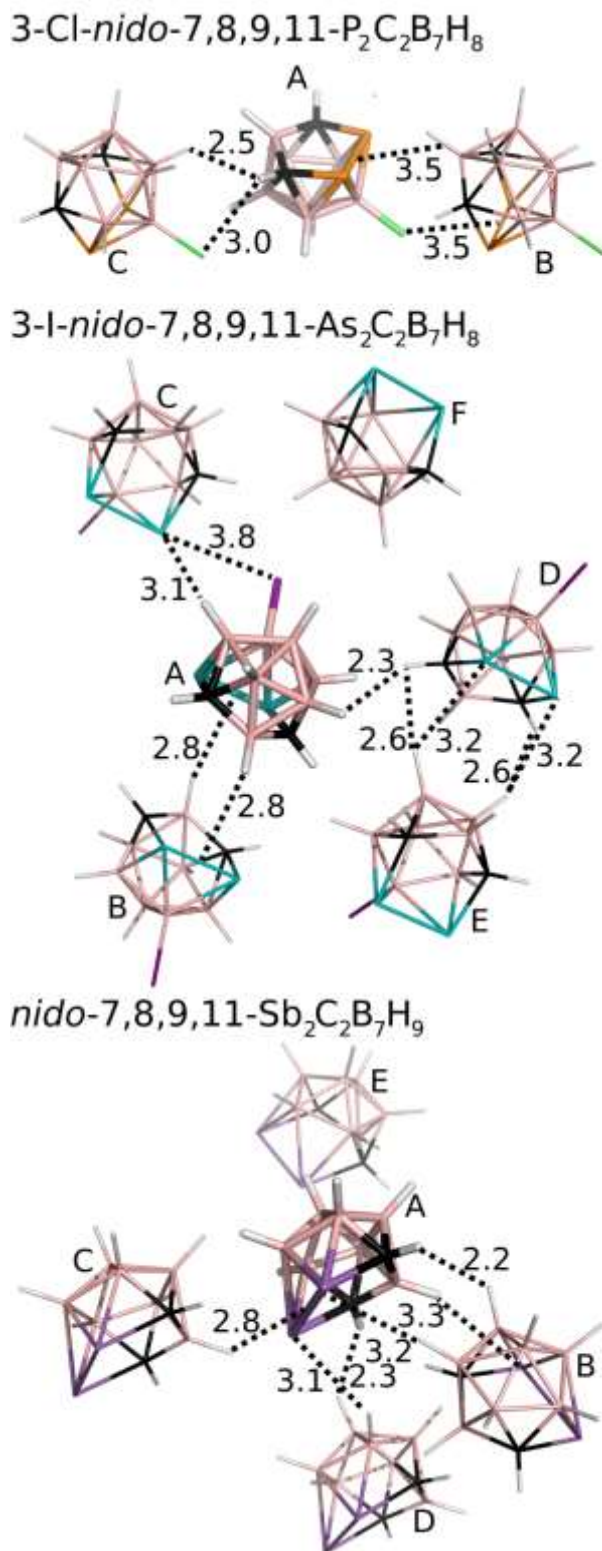
The crystal structure of **3** has two binding motifs with  $\Delta E$  exceeding  $-6 \text{ kcal mol}^{-1}$ . The A $\cdots$ B motif has  $\Delta E$  of  $-7.1 \text{ kcal mol}^{-1}$  and is stabilized by multiple interactions, specifically by two Sb $\cdots$ H-B Pn-bonds and one C-H $\cdots$ H-B HH-bond. On the other side, the A $\cdots$ C motif is exclusively formed by a single interaction, namely a Sb $_2\cdots$ H-B Pn-bond.  $\Delta E$  of  $-6.5 \text{ kcal mol}^{-1}$  computed for this binding motif can thus be considered as  $\Delta E$  of the isolated Pn-bond. This is a very large value, exceeding  $\Delta E$  of isolated Pn-bonding of **2** by about 100%. The Pn-bonding of **3** is even slightly more favorable than Pn-bonding in Cl $_3$ Sb $\cdots$ N(Me) $_3$  and Cl $_3$ Sb $\cdots$ benzene complexes ( $\Delta E$  of  $-5.8$  and  $-6.1 \text{ kcal mol}^{-1}$ , respectively).<sup>15</sup>

**Table 3.** Interaction energies ( $\Delta E$ ) in  $\text{kcal mol}^{-1}$ .

	Interaction	MP2.5/CCSD(T)
<b>3-Cl-nido-7,8,9,11-P<math>_2</math>C<math>_2</math>B<math>_7</math>H<math>_8</math></b>		
A $\cdots$ B	2 $\times$ Pn-bonds	$-5.93/-6.10$
A $\cdots$ C	H- and HH-bonds	$-4.19/-4.39$
<b>3-I-nido-7,8,9,11-As<math>_2</math>C<math>_2</math>B<math>_7</math>H<math>_8</math></b>		
A $\cdots$ B	2 $\times$ Pn-bonds	$-5.98$
A $\cdots$ C	2 $\times$ Pn-bonds	$-5.67$
D $\cdots$ E	Pn- and HH-bonds	$-4.52$
A $\cdots$ D	HH-bond	$-3.52$
A $\cdots$ F	Stacking	$-2.66$
<b>nido-7,8,9,11-Sb<math>_2</math>C<math>_2</math>B<math>_7</math>H<math>_9</math></b>		
A $\cdots$ B	2 $\times$ Pn-bond, HH-bond	$-6.80/-7.05$
A $\cdots$ C	Single Pn-bond	$-6.22/-6.46$
A $\cdots$ D	HH-bond, Pn-bond	$-4.79$
A $\cdots$ E	Stacking	$-4.10$



**Figure 4.** The most significant/stable interaction motifs from the crystalline structures of 3-Cl-*nido*-7,8,9,11-P<sub>2</sub>C<sub>2</sub>B<sub>7</sub>H<sub>8</sub> (**1**), 3-I-*nido*-7,8,9,11-As<sub>2</sub>C<sub>2</sub>B<sub>7</sub>H<sub>8</sub> (**2**), and *nido*-7,8,9,11-Sb<sub>2</sub>C<sub>2</sub>B<sub>7</sub>H<sub>9</sub> (**3**). Distances are in Å. The color coding as follows: pink – B; black – C; orange – P; green – Cl; white – H; cyan – As; purple – I; magenta – Sb. Positions of H atoms were optimized at the DFT-D3/BLYP/DZVP level.<sup>11</sup>



## Methods

### Synthesis

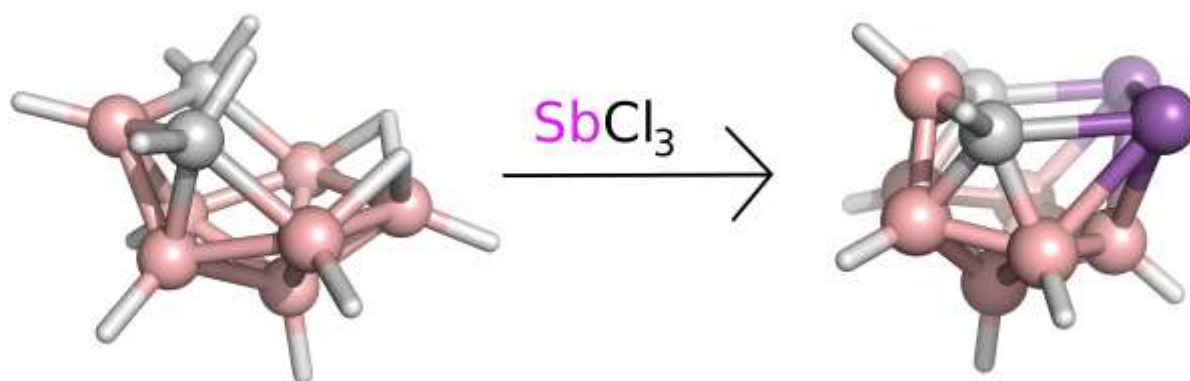


**Figure 5.** The reaction scheme of *arachno*-4,6-C<sub>2</sub>B<sub>7</sub>H<sub>13</sub> with SbCl<sub>3</sub> yielding the *nido*-7,8,9,11-Sb<sub>2</sub>C<sub>2</sub>B<sub>7</sub>H<sub>9</sub> compound.

A solution of *arachno*-4,6-C<sub>2</sub>B<sub>7</sub>H<sub>13</sub> (0.226 g, 2 mmol, see also Figure 5) in dichloromethane (20 mL) was treated with proton-sponge (1.5 g, 7 mmol). SbCl<sub>3</sub> (2.0 g, 16 mmol) was added under stirring and cooling to 0 °C (see Scheme 1). Stirring was continued at room temperature for 4 h and the mixture was then cooled to 0 °C and decomposed by the dropwise addition of water (20 mL). Column chromatography was carried out on silica gel as the stationary phase (3 g). The solids were mounted onto a silica gel column and the column was eluted with dichloromethane. The chromatography led to the separation of a major yellow fraction of  $R_f = 0.73$  (CH<sub>2</sub>Cl<sub>2</sub>), which was evaporated to dryness. 0.255 g of yellowish *nido*-7,8,9,11-Sb<sub>2</sub>C<sub>2</sub>B<sub>7</sub>H<sub>9</sub> was obtained (yield 36%, with respect to the starting material 4,6-C<sub>2</sub>B<sub>7</sub>H<sub>13</sub>).

### Computational modeling

Magnetic shielding was calculated using the GIAO-MP2 method incorporated into Gaussian09<sup>16</sup> utilizing the IGLO-II basis with the MP2/cc-pVTZ geometry (with TZVP basis set on Sb by Weigend<sup>17</sup> with ECP by Metz<sup>18</sup>) and frozen core electrons. Electrostatic potentials were computed at the HF/cc-pVDZ level (for I basis set in Ref. 19) using Gaussian09 and Molekel4.3<sup>20</sup> programs. It has recently been shown that this basis set size is sufficient for these purposes.<sup>21</sup>

Interaction energy ( $\Delta E$ ) values were calculated for all pairwise interactions the crystal structures of **1**, **2** and **3**. All hydrogen atoms were optimized using DFT-D3/BLYP/DZVP method prior the energy calculations.<sup>11</sup>  $\Delta E$  for the central molecule with each surrounding molecule was evaluated at MP2.5/CBS using the Turbomole 6.6<sup>22</sup> and Cuby4<sup>23</sup> programs. MP2.5/CBS was calculated as the sum of MP2/CBS energy and MP2.5 correction. MP2/CBS was approximated by RI-MP2-F12/cc-pVTZ-F12 for **1**.<sup>24</sup> In the case of **2** and **3**, we used MP2 extrapolation to the CBS from cc-pVTZ to cc-pVQZ (for I and Sb atoms cc-pVTZ-PP and cc-pVQZ-PP pseudopotentials were used).<sup>25</sup> The MP2.5 correction term was calculated using the aug-cc-pVDZ basis set. MP2.5/CBS interaction energies were compared to benchmark CCSD(T)/CBS for the interaction motifs of **1** and the most favourable motifs of **3**. The CCSD(T)/CBS correction term was also determined using the aug-cc-pVDZ basis sets. Counterpoise corrections for basis set superposition error (BSSE) are used for all energy calculations.

### Crystallography

Full sets of diffraction data for **3** were collected at 150(2) K using a Bruker D8-Venture diffractometer equipped with Mo ( $\text{Mo}/\text{K}\alpha$  radiation;  $\lambda = 0.71073 \text{ \AA}$ ) microfocus X-ray ( $\text{I}\mu\text{S}$ ) source, Photon CMOS detector and Oxford Cryosystems cooling device was used for data collection.

The frames were integrated using the Bruker SAINT software package using a narrow-frame algorithm. Data were corrected for absorption effects using the Multi-Scan method (SADABS). Data were treated by XT-version 2014/5 and SHELXL-2014/7 software implemented in APEX3 v2016.5-0 (Bruker AXS) system.<sup>26</sup> Hydrogen atoms were mostly localized on a difference Fourier map; however, to ensure uniformity of treatment of the crystal, all hydrogen atoms were recalculated into idealized positions (riding model) and assigned temperature factors  $H_{\text{iso}}(\text{H}) = 1.2 U_{\text{eq}}$  (pivot atom). H atoms in were placed with C-H distances of 1.1  $\text{\AA}$  for B-H and C-H bonds in the carborane cage. Hydrogen atoms in the upper rim of the cage were placed according to the appropriate maxima found on the Fourier difference electron density map.

$R_{\text{int}} = \frac{\sum |F_o^2 - F_{o,\text{mean}}^2|}{\sum F_o^2}$ ,  $S = [\frac{\sum (w(F_o^2 - F_c^2)^2)}{(N_{\text{diffrs}} - N_{\text{params}})}]^{1/2}$  for all data,  $R(F) = \frac{\sum ||F_o| - |F_c||}{\sum |F_o|}$  for observed data,  $wR(F^2) = [\frac{\sum (w(F_o^2 - F_c^2)^2)}{(\sum w(F_o^2)^2)}]^{1/2}$  for all data.

Crystallographic data for structural analysis have been deposited with the Cambridge

Crystallographic Data Centre, CCDC no. 1553208 for **3**. Copies of this information may be obtained free of charge from The Director, CCDC, 12 Union Road, Cambridge CB2 1EY, UK (fax: +44-1223-336033; e-mail: deposit@ccdc.cam.ac.uk or www: <http://www.ccdc.cam.ac.uk>).

Crystallographic data and structural refinement parameters for colorless single crystals of **3**:  $C_2H_9B_7Sb_2$ ,  $M = 352.26 \text{ g mol}^{-1}$ , orthorhombic,  $Pna2_1$ ,  $a = 20.4799(12)$ ,  $b = 6.6471(4)$ ,  $c = 6.5803(4) \text{ \AA}$ ,  $\beta = 90^\circ$ ,  $Z = 4$ ,  $V = 895.79(9) \text{ \AA}^3$ ,  $D_c = 2.612 \text{ g cm}^{-3}$ ,  $\mu = 5.946 \text{ mm}^{-1}$ ,  $T_{\min}/T_{\max} = 0.583/0.745$ ;  $-27 \leq h \leq 27$ ,  $-8 \leq k \leq 8$ ,  $-8 \leq l \leq 8$ ; 19233 reflections measured ( $\theta_{\max} = 28.35^\circ$ ), 2223 independent ( $R_{\text{int}} = 0.1199$ ), 1796 with  $I > 2\sigma(I)$ , 106 parameters,  $S = 1.049$ ,  $RI(\text{obs. data}) = 0.0271$ ,  $wR2(\text{all data}) = 0.0398$ ; max., min. residual electron density = 1.091,  $-1.107 \text{ e \AA}^{-3}$ .

## Conclusions

To sum up, in compound **3** (*nido*-7,8,9,11- $Sb_2C_2B_7H_9$ ) we have synthesized and crystallized the very first reported cluster containing simultaneously Sb-B, Sb-C and Sb-Sb covalent bonds. In addition to that, the distance between two Sb atoms in the open pentagonal belt of **3** is less than the sum of Sb covalent radii. Further quantum chemical analysis revealed that the most stable crystal motifs in the crystal structure of **3** were directed by Pn-bonding.  $\Delta E$  of a very strong  $Sb \cdots H-B$  Pn-bond would exceed  $-6.0 \text{ kcal mol}^{-1}$ . For comparison, the Pn-bonding in **3** is more favorable than the reported Pn-bonding in  $Cl_3Pn \cdots N(Me)_3$  and is comparable to the Pn-bonding in  $Cl_3Pn \cdots \pi$  complexes (Pn = As, Sb). Phosphorus and arsenic can occupy the same positions as Sb in **3**. However, in contrast to **3**, crystallization of the parent *nido*-7,8,9,11- $Pn_2C_2B_7H_8$  (Pn = P, As) has not been possible. Indeed, crystal packing of halogenated 3-*X-nido*-7,8,9,11- $Pn_2C_2B_7H_8$  (X = Cl or I; Pn = P, As) derivatives is also dominated by Pn-bonding. We believe that Pn-bonding of *nido*-7,8,9,11- $Pn_2C_2B_7H_9$ -type compounds offers a tantalizing possibility to further examine the pnictogen bonding in a very detailed manner.

## Acknowledgement

This work was supported by the research project RVO 61388963 of the Czech Academy of Sciences. We acknowledge the financial support of the Czech Science Foundation (17-08045S).

## References

- 1 (a) W. N. Lipscomb, *Boron Hydrides*, Benjamin, New York, 1963; (b) D. Hnyk and D. A. Wann, *Boron – the Fifth Element*, Chapter 2, Challenges and Advances in Computational Chemistry and Physics, Vol 20, (Eds. D. Hnyk and M. McKee), Springer, Heidelberg, New York, Dordrecht and London, 2015.
- 2 K. Wade, *Nat. Chem.*, 2009, **1**, 92.
- 3 (a) J. I. Little, *Inorg. Chem.*, 1979, **18**, 1598; (b) L. J. Todd, A. R. Burke, A.R. Garber, H.T. Silverstein and B.N. Storhoff, *Inorg. Chem.*, 1970, **9**, 2175. Note that HOMO of  $(\text{Me}_2\text{PPh})_2\text{Pd}^{(2+)}$  and SLUMO (the second lowest unoccupied orbital) of the  $\text{B}_9\text{H}_9\text{Sb}_2^{(2-)}$  accounts for the stabilization.
- 4 S. A. Jasper, Jr., S. Roach, J. N. Stipp, J. C. Huffman and L. J. Todd, *Inorg. Chem.*, 1993, **32**, 3072.
- 5 R. N. Grimes, *Angew. Chem. Int. Ed.*, 2003, **42**, 1198. The interaction of the suitable symmetrical *d* orbitals of a metal with HOMO of the borane-cluster fragment is a driving force for the origination of the metallocarboranes.
- 6 J. Holub, T. Jelínek, D. Hnyk, Z. Plzák, I. Císařová, M. Bakardjiev and B. Štíbr, *B. Chem. Eur. J.*, 2001, **7**, 1546.
- 7 L. Mikulášek, B. Grüner, I. Císařová and B. Štíbr, *B. Dalton Trans.*, 2003, **7**, 1332.
- 8 (a) W. Wang, W. Wang and W. J. Jin, *Chem. Rev.*, 2016, **116**, 5072; (b) A. Bauza, T. J. Mooibroek and A. Frontera, *ChemPhysChem*, 2015, **16**, 2496.
- 9 T. Clark, M. Hennemann, J. S. Murray and P. Politzer, *J. Mol. Model.*, 2007, **13**, 291.
- 10 (a) J. Fanfrlík, A. Páda, Z. Padělková, A. Pecina, J. Macháček, M. Lepšík, J. Holub, A. Růžička, D. Hnyk and P. Hobza, *Angew. Chem. Int. Ed.*, 2014, **53**, 10139; (b) J. Fanfrlík and D. Hnyk, *CrystEngComm*, 2016, **18**, 8973.
- 11 J. Fanfrlík, J. Holub, Z. Růžičková J. Řezáč, P. D. Lane, D. A. Wann, D. Hnyk, A. Růžička and P. Hobza, *ChemPhysChem.*, 2016, **17**, 3373.
- 12 D. Hnyk, E. Vajda, M. Bühl and P. v. R. Schleyer, *Inorg. Chem.*, 1992, **31**, 2464. For the mechanism of the antipodal effect, see D. Hnyk, D. A. Wann, J. Holub, S. Samdal and D. W. H. Rankin, *Dalton Trans.*, 2011, **40**, 5734.
- 13 P. v. R. Schleyer, Ch. Maerker, A. Dransfeld, H. Jiao and N. J. R. v. Eikema Hommes, *J. Am. Chem. Soc.*, 1996, **118**, 6317.

- 14 (a) P. Pyykkö and M. Atsumi, *Chem. Eur. J.*, 2009, **15**, 186; b) W. Lu, H. Hu, Y. Li, R. Ganguly and R. Kinjo, *J. Am. Chem. Soc.*, 2016, 138, 6650; (c) C. R. Wade, M. R. Saber and F. P. Gabbai, *Heteroat. Chem.*, 2011, 22, 500.
- 15 A. Bauza, D Quinonero, P. M. Deya and A. Frontera, *CrystEngComm*, 2013, **15**, 3137.
- 16 M. J. Frisch, G. W. Trucks, H. B. Schlegel, G. E. Scuseria, M. A. Robb, J. R. Cheeseman, G. Scalmani, V. Barone, B. Mennucci, G. A. Petersson, H. Nakatsuji, M. Caricato, X. Li, H. P. Hratchian, A. F. Izmaylov, J. Bloino, G. Zheng, J. L. Sonnenberg, M. Hada, M. Ehara, K. Toyota, R. Fukuda, J. Hasegawa, M. Ishida, T. Nakajima, Y. Honda, O. Kitao, H. Nakai, T. Vreven, J. A. Montgomery, Jr., J. E. Peralta, F. Ogliaro, M. Bearpark, J. J. Heyd, E. Brothers, K. N. Kudin, V. N. Staroverov, R. Kobayashi, J. Normand, K. Raghavachari, A. Rendell, J. C. Burant, S. S. Iyengar, J. Tomasi, M. Cossi, N. Rega, J. M. Millam, M. Klene, J. E. Knox, J. B. Cross, V. Bakken, C. Adamo, J. Jaramillo, R. Gomperts, R. E. Stratmann, O. Yazyev, A. J. Austin, R. Cammi, C. Pomelli, J. W. Ochterski, R. L. Martin, K. Morokuma, V. G. Zakrzewski, G. A. Voth, P. Salvador, J. J. Dannenberg, S. Dapprich, A. D. Daniels, Ö. Farkas, J. B. Foresman, J. V. Ortiz, J. Cioslowski and D. J. Fox, Gaussian, Inc., Wallingford CT, 2009.
- 17 F. Weigend and R. Ahlrichs, *Phys. Chem. Chem. Phys.*, 2005, **7**, 3297.
- 18 In-Sb(ecp-28): B. Metz, H. Stoll and M. Dolg, *J. Chem. Phys.*, 2000, **113**, 2563.
- 19 A. Bergner, M. Dolg, W. Küchle, H. Stoll and H. Preuss, *Mol. Phys.*, 1993, **80**, 1431.
- 20 a) MOLEKEL 4.3, P. Flükiger, H. P. Lüthi, S. Portmann and J. Weber, Swiss Center for Scientific Computing, Manno (Switzerland), 2000; b) S. Portmann, H. P. Lüthi. MOLEKEL: CHIMIA, 2007, **28**, 555.
- 21 K. E. Riley, K.-A. Tran, P. Lane, J. S. Murray and P. Politzer, *J. Comput. Sci.*, 2016, **17**, 273.
- 22 R. Ahlrichs *et al.*, TURBOMOLE V6.2 2010, a development of the University of Karlsruhe and Forschungszentrum Karlsruhe GmbH, 1989–2007, TURBOMOLE GmbH, since 2007; available from <http://www.turbomole.com>. *Turbomole V6*, Karlsruhe, Deutschland, 2008.
- 23 J. Řezáč, *J. Comput. Chem.* 2016, **37**, 1230.
- 24 K. A. Peterson, T. B. Adler and H.-J. Werner, *J. Chem. Phys.*, 2008, **128**, 084102.

- 25 A. Halkier, T. Helgaker, P. Jørgensen, W. Klopper, H. Koch, J. Olsen and A. K. Wilson, *Chem. Phys. Lett.*, 1998, **286**, 243.
- 26 G. M. Sheldrick, *Acta Cryst.* 2015, A71, 3-8.

## Graphical abstract

The reaction of *arachno*-4,6-C<sub>2</sub>B<sub>7</sub>H<sub>13</sub> with SbCl<sub>3</sub> yields the *nido*-7,8,9,11-Sb<sub>2</sub>C<sub>2</sub>B<sub>7</sub>H<sub>9</sub> compound, which simultaneously has Sb-Sb, Sb-B and Sb-C bonds and a unique ability to form pnictogen bonds.

